INT. J. NUM. METH. HEAT FLUID FLOW, VOL. 6, NO. 7, 63–80 (1996)

APPROXIMATE ANALYTICAL SOLUTIONS FOR DIFFUSION PROBLEMS IN UNBOUNDED MEDIA AND THEIR APPLICATION IN INFINITE ELEMENTS

Y.C. LI

Department of Civil Engineering, Shanghai Tiedao University, Shanghai 200333, People's Republic of China

ABSTRACT

This paper presents approximate analytical solutions for the diffusion problems of a cylindrical hole in an infinite medium and a slot in an infinite medium with properly prescribed boundary conditions and initial conditions. These solutions have much simpler forms than those of exact analytical solutions, and asymptotically approach the exact solutions with increasing time or the material point moving away from the internal boundary. The approximate analytical solution for the diffusion problem of a slot in an infinite medium is applied to establish a shape function for the infinite elements. Good agreement is found in comparison of our results with those presented by Li and Huang and Cinco-Ley *et al.* Finally, an example simulating a primary recovery procedure in hydraulic fracturing technique for an oil field is presented.

KEY WORDS Diffusion Elements Infinite Approximate Analytical Solutions

INTRODUCTION

Boundary-valued diffusion problems in unbounded media are of important significance in engineering practice, especially in geotechnical engineering applications. It is well-known that both thermal conduction and seepage problems are in the class of diffusion problems. Oil recovery and underground water recovery are the examples of seepage problems, in which the boundaries of pay-zones are usually unknown but far from the production wells. Artificial ground freezing and geothermal energy extraction can be the examples of thermal conduction problems, in which the regions to be analysed are of small dimensions in comparison with the surrounding media. It is natural to idealize these problems as the interested areas in infinite domains.

In the conventional finite element method for diffusion problems, an infinite domain is replaced by a sufficiently large domain. The boundary value defined on the internal boundary is supposed to have a negligible influence on the outer boundary of the domain. Results obtained are generally good for the case of small time. However, with the increasing time, the internal boundary value will perturb the outer boundary eventually, no matter how large the finite domain is. Furthermore, a large number of nodal points may be involved in analysing the large domain.

Jaeger[1] provided an analytical solution of temperature field for radial heat flow problems. He studied the case of a cylindrical hole located in an infinite medium with a prescribed constant temperature on the hole boundary or a prescribed constant flow rate of heat in the hole. This solution is expressed in a singular integral form. Kucuk and Brigham[2] presented an analytical solution for the problem of a slot located in an infinite medium with a prescribed constant pressure on the slot surface or a prescribed constant flow rate in the slot. Li and Huang[3] presented an extrapolation method to estimate the solution for an infinite medium. This method extrapolates a

0961–5539

Received June 1995
Revised September 1995

series of solutions of finite media by means of the finite element method to find the solution for the infinite medium. With the use of Green's function, Cinco-Ley *et al.*[4] developed a semi-analytical method to estimate the solution for the problem of a rectangular finite conductivity fracture in an infinite medium.

In the past few decades, research effort has been expanded in developing infinite elements, which are well suited to modelling the remote region in the unbounded medium. The pioneer work in this field might have been done in the 1970s[5-8]. This method has been developed by several authors afterwards. The infinite elements can be classified into two categories:

(1) the infinite elements in which the shape functions are expressed in some decay functions with the distance from the material point to the decaying origin approaching infinity, e.g. the shape functions with $1/r^n$ type decay or exponential type decay[5,9-11]. Integration in the infinite elements based on the decay functions results in finite values;

(2) the infinite elements which are mapped onto finite parent elements with local co-ordinate parameters[12-15]. After mapping, the shape functions in the infinite elements can be expressed in a set of polynomial terms varying as $1/r$, $1/r^2$, $1/r^3$, etc. The advantage of this approach is that the integration in the infinite elements can be proceeded in the finite parent elements. Algorithms for the mapped infinite elements follow the finite element procedure so closely that they can be readily implemented into existing finite element programmes. If the shape functions can well depict the behaviour of the physical quantities in the infinite region, good results are usually obtained. The infinite elements based on these shape functions are extensively used in analyses of stress/displacement problems, diffusion problems, wave propagation problems, etc. in unbounded media.

In this paper, approximate analytical solutions for the diffusion problems which were solved by Jaeger[1] for thermal conduction problems, and by Kucuk *et al.*[2] for seepage problems are presented. These approximate solutions have much simpler closed forms than their solutions. These approximate analytical solutions are applied to establish shape functions for the infinite elements for the problem of a conductive fracture in an infinite medium. The results are compared with those presented by Li and Huang[3] and Cinco-Ley *et al.*[4]. Results for a seepage problem of a conductive vertical fracture with an elliptic shape in an infinite slab reservoir are presented as an example.

APPROXIMATE ANALYTICAL SOLUTIONS

Since both thermal conduction problem and seepage problem belong to the class of diffusion problems, the two problems will not be distinguised in the following, but are generally called diffusion problems.

A single well in an infinite medium

The differential equation for axially symmetric diffusion problems can be expressed, in a cylindrical polar co-ordinate system, as:

$$\frac{\partial^2 \phi}{\partial r^2} + \frac{1}{r}\frac{\partial \phi}{\partial r} - \frac{1}{\kappa}\frac{\partial \phi}{\partial t} = 0 \tag{1}$$

where

ϕ = Pore pressure for seepage, or temperature for heat conduction

r = Polar radius

t = Time

κ = Coefficient of diffusion. $\kappa = \frac{k}{\rho c}$ for heat conduction and $\kappa = \frac{K}{c}$ for seepage

k = Coefficient of heat conduction

ρ = Mass density

c = Special heat for heat conduction, or compressibility of fluid for seepage

K = Permeability coefficient of the medium

The function of ϕ is independent of polar angle θ because of the axial symmetry.

The initial condition is

$$\phi(r,0) = \phi_0 \tag{2}$$

where ϕ_0 is an initial constant value of ϕ. The boundary condition on the hole wall is:

$$\phi(a,t) = \phi_w \tag{3}$$

or

$$\frac{\partial}{\partial r}\phi(a,t) = \phi_w' \tag{4}$$

where a is the radius of the hole, ϕ_w and ϕ_w' are given constants. The condition at infinity is:

$$\lim_{r\to\infty} \phi(r,t) = \phi_0 \tag{5}$$

Let us take the trial function:

$$\phi = (\phi_w - \phi_0)\frac{\mathrm{Ei}\left(\frac{r^2}{4\kappa t}\right)}{\mathrm{Ei}\left(\frac{a^2}{4\kappa t}\right)} + \phi_0 \tag{6}$$

where Ei is the exponential integral. It can be easily proved that function ϕ in equation (6) satisfies the initial condition, equation (2), internal boundary condition, equation (3), and the limiting condition, equation (5). The trial function ϕ does not satisfy differential equation (1). However, substituting ϕ into equation (1), we find that the residual of the left-hand side of equation (1) vanishes for large time t or large radius r. Thus, function ϕ in equation (6) is a good approximate solution for large t or r.

The exact solution presented by Jaeger[1] is:

$$\phi = (\phi_w - \phi_0)\left[1 + \frac{2}{\pi}\int_0^\infty e^{-\kappa u^2 t}\frac{J_0(ur)Y_0(ua) - Y_0(ur)J_0(ua)}{J_0^2(ua) + Y_0^2(ua)}\frac{du}{u}\right] + \phi_0 \tag{7}$$

where J_0 and Y_0 are respectively the first and second kinds of Bessel functions of order zero. Numerical results of equation (7) are given in a dimensionless form of ϕ_D against t_D (*Figure 1*), where

$$\phi_D = \frac{\phi - \phi_0}{\phi_w - \phi_0} \tag{8}$$

$$t_D = \frac{\kappa t}{a^2} \tag{9}$$

Then the values of ϕ_D are calculated against t_D according to equation (6) and compared with the exact solution by Jaeger as shown in *Figure 1*. The tendency that the approximate analytical solution approaches the exact solution with increasing time t or radius r can be clearly seen.

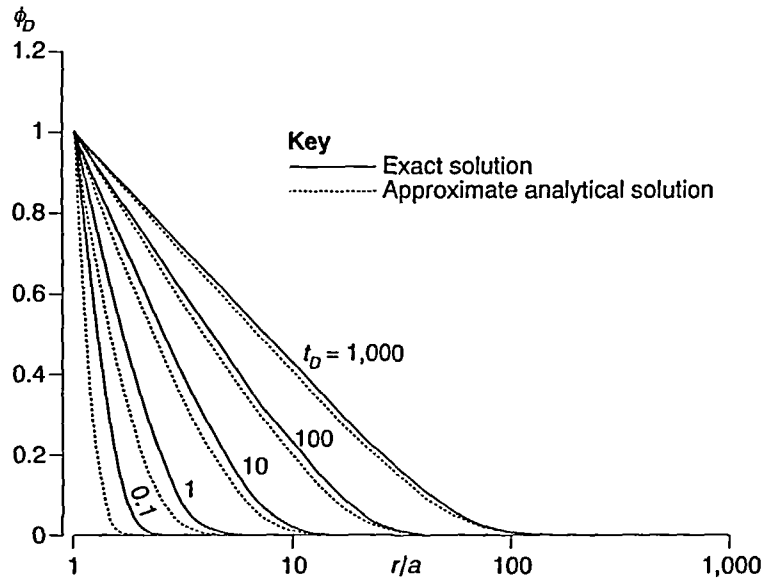

Figure 1 Comparison of the approximate analytical solution of temperature ϕ_D with the exact solution by Jaeger[1]. Case: A cylindrical hole in an infinite medium with a prescribed constant temperature on the hole wall

Although equation (6) is merely an approximate solution, it has a much simpler form than the exact solution, equation (7).

Second, let us investigate another function:

$$\phi = -\frac{1}{2} a\phi_w' \,\mathrm{Ei}\left(\frac{r^2}{4\kappa t}\right) \exp\left(\frac{a^2}{4\kappa t}\right) + \phi_0 \tag{10}$$

If the flow rate q is prescribed for the seepage problem, equation (10) can be rewritten as:

$$\phi = \frac{q}{4\pi K h} \,\mathrm{Ei}\left(\frac{r^2}{4\kappa t}\right) \exp\left(\frac{a^2}{4\kappa t}\right) + \phi_0 \tag{11}$$

where h is the thickness of the medium. The flow rate q is defined positive for flowing into the medium. It can be found that function ϕ in equation (10) satisfies the initial condition, equation (2), internal boundary condition, equation (4) and the limiting condition, equation (5). Substituting ϕ as shown in equation (10) into equation (1), it can be found that the residual of the left-hand side of equation (1) vanishes if r or t approaches infinity.

A slot in an infinite medium

Set the origin of the Cartesian co-ordinate system at the centre of the slot and the x-axis parallel to the slot. The differential equation of the diffusion problem can be expressed as:

$$\frac{\partial^2\phi}{\partial x^2} + \frac{\partial^2\phi}{\partial y^2} - \frac{1}{\kappa}\frac{\partial\phi}{\partial t} = 0 \tag{12}$$

Employing the following transforms:

$$\left.\begin{aligned} x &= L\cosh\xi\cos\eta \\ y &= L\sinh\xi\sin\eta \end{aligned}\right\} \tag{13}$$

equation (12) becomes:

$$\frac{\partial^2\phi}{\partial\xi^2}+\frac{\partial^2\phi}{\partial\eta^2}-\frac{1}{\kappa}L^2(\cosh^2\xi-\cos^2\eta)\frac{\partial\phi}{\partial t}=0 \tag{14}$$

where L is the half length of the slot, ξ and η are the elliptical co-ordinates. The exact solution of equation (14) was given by Kucuk[2] as

$$\phi_D(\xi,\eta;t_D)=1+\frac{2}{\pi}\sum_{n=0}^{\infty}\int_0^{\infty}\exp(-4\lambda t_D)\cdot$$

$$A_0^{(2n)}(\lambda)\left[\frac{\mathrm{Ce}_{2n}(\xi,\lambda)\mathrm{Fey}_{2n}(\xi_w,\lambda)-\mathrm{Fey}_{2n}(\xi,\lambda)\mathrm{Ce}_{2n}(\xi_w,\lambda)}{\mathrm{Ce}_{2n}^{\ 2}(\xi_w,\lambda)+\mathrm{Fey}_{2n}^{\ 2}(\xi_w,\lambda)}\right]\mathrm{ce}_{2n}(\eta,\lambda)\frac{\mathrm{d}\lambda}{\lambda} \tag{15}$$

where

λ = Integral parameter

$A_0^{(2n)}(\lambda)$ = Fourier coefficient

$\mathrm{Ce}_{2n}(\xi,\lambda)$, $\mathrm{Fey}_{2n}(\xi,\lambda)$ and $\mathrm{ce}_{2n}(\eta,\lambda)$ = Matthieu functions

ξ_w = The value of ξ on the slot surface, here $\xi_w = 0$

t_D = The dimensionless time defined by:

$$t_D=\frac{\kappa t}{L^2} \tag{16}$$

Obviously, it is very difficult to carry out the integration as shown in equation (15). In the following, we will search for an approximate solution.

For large ξ, we have $\cosh\xi >> \cos\eta$ and $\cosh\xi \approx \sinh\xi \approx \frac{1}{2}e^{\xi}$. Hence, equation (14) can be approximately rewritten as:

$$\frac{\partial^2\phi}{\partial\xi^2}+\frac{\partial^2\phi}{\partial\eta^2}-\frac{1}{\kappa}L^2\frac{e^{2\xi}}{4}\frac{\partial\phi}{\partial t}=0 \qquad \text{for large } \xi \tag{17}$$

The initial condition can be written as:

$$\phi(\xi,\eta;0)=\phi_0 \tag{18}$$

The boundary condition on the slot surface is:

$$\phi(0,\eta;t)=\phi_w \tag{19}$$

Function ϕ should satisfy the limiting condition at infinity, i.e.

$$\lim_{\xi\to\infty}\phi(\xi,\eta;t)=\phi_0 \tag{20}$$

It can be easily proved that function:

$$\phi=(\phi_w-\phi_0)\frac{\mathrm{Ei}\left(\frac{e^{2\xi}}{16t_D}\right)}{\mathrm{Ei}\left(\frac{1}{16t_D}\right)}+\phi_0 \tag{21}$$

satisfies conditions, equations (18), (19) and (20), and the residual term of equation (17) approaches zero for large ξ or t when substituting the function into equation (17). Hence, function

ϕ shown as equation (21) is a good approximate solution for large ξ or t. It is noted that equation (21) does not include parameter η. It means that the distribution of ϕ on any constant ξ-curve for large ξ is uniform.

According to equation (21), the flow rate in the slot can be expressed as:

$$q = -4Kh \int_0^L \frac{\partial \phi}{\partial y}\bigg|_{\xi=0} dx = 4Kh \frac{\pi(\phi_w - \phi_0)}{\mathrm{Ei}\left(\frac{1}{16t_D}\right)} \exp\left(-\frac{1}{16t_D}\right) \tag{22}$$

Let us employ the dimensionless forms of the flow rate used by Kucuk[2]:

$$q_D = \frac{q}{2\pi Kh(\phi_w - \phi_0)} = 2\left[\mathrm{Ei}\left(\frac{1}{16t_D}\right)\right]^{-1} \exp\left(-\frac{1}{16t_D}\right) \tag{23}$$

Kucuk[2] presented the numerical results of q_D against t_D using his exact analytical solution, equation (15). In *Figure 2* the results of q_D from equation (23) are plotted and compared with those presented by Kucuk. It is found that the two q_D's have large difference initially, nevertheless they are close to each other gradually and finally nearly the same.

For presented constant flow rate q, it can be proved that a good approximate analytical solution for large ξ or t can be obtained as:

$$\phi = \frac{q}{4\pi Kh} \mathrm{Ei}\left(\frac{e^{2\xi}}{16t_D}\right) \exp\left(\frac{1}{16t_D}\right) + \phi_0 \tag{24}$$

Kucuk[2] employed the dimensionless form of ϕ as:

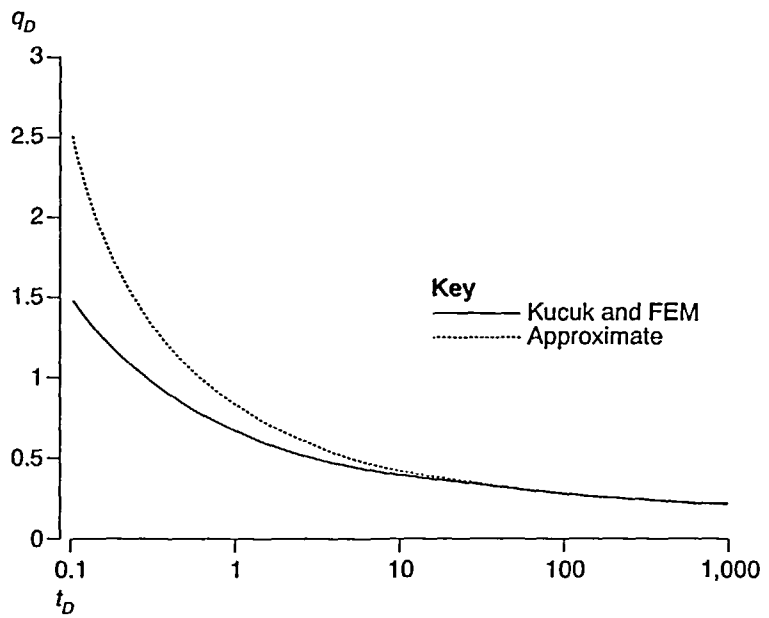

Figure 2 Flow rate q_D at the well bore vs time t_D for the case of a slot in an infinite medium with a prescribed constant pressure on the slot surface

$$\phi_D = \frac{2\pi Kh(\phi - \phi_0)}{q} \tag{25}$$

With the use of equations (24) and (25), we have the expression of the dimensionless form of ϕ_D on the slot surface as:

$$\phi_{wD} = \frac{1}{2}\,\mathrm{Ei}\left(\frac{1}{16t_D}\right)\exp\left(\frac{1}{16t_D}\right) \tag{26}$$

which is the inverse of equation (23). Comparing the numerical results of ϕ_{wD} as shown in equation (26) with those presented by Kucuk[2], it is found that the results of this study are close to Kucuk's results for large t_D (*Figure 3*).

THE FINITE AND INFINITE ELEMENTS METHOD FOR A SLOT IN AN INFINITE MEDIUM

For the diffusion problem of a slot in an infinite medium, our approximate analytical solution is not good for small time t or small distance from material point to the slot. In this case, the finite element method can make it up. The domain of the diffusion problem should be so large that on the outer boundary we have $e^{2\xi} >> 1$. The boundary condition on the outer boundary can be determined by the approximate analytical solution, equation (21) or (24). This method is equivalent to that of employing an infinitely large element outside the finite domain (*Figure 4*). However the latter is more effective than the former, especially in the case that the value of ϕ varies on the slot surface.

First, let us use a two-step backward finite difference equation with variable time increment to approximate the time-derivative in equation (12), i.e.

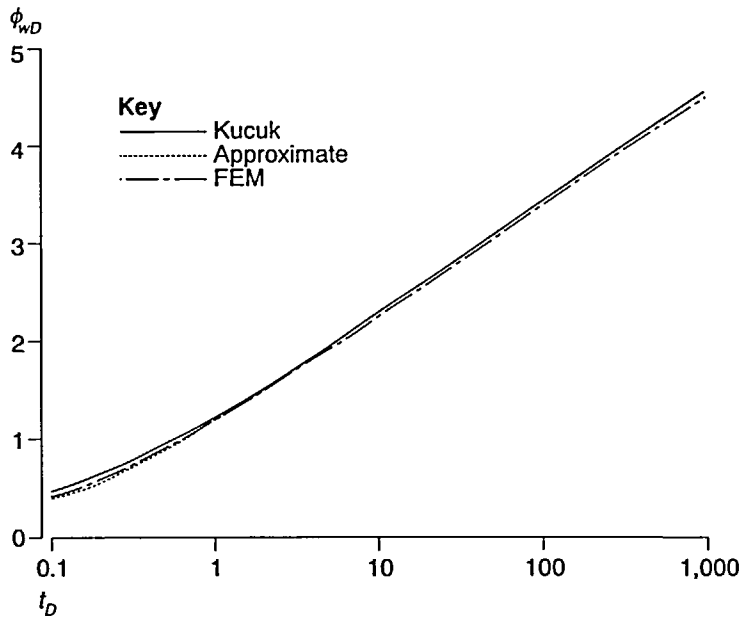

Figure 3 Pressure ϕ_{wD} on the slot surface vs time t_D for the case of a slot in an infinite medium with a prescribed flow rate at the well bore

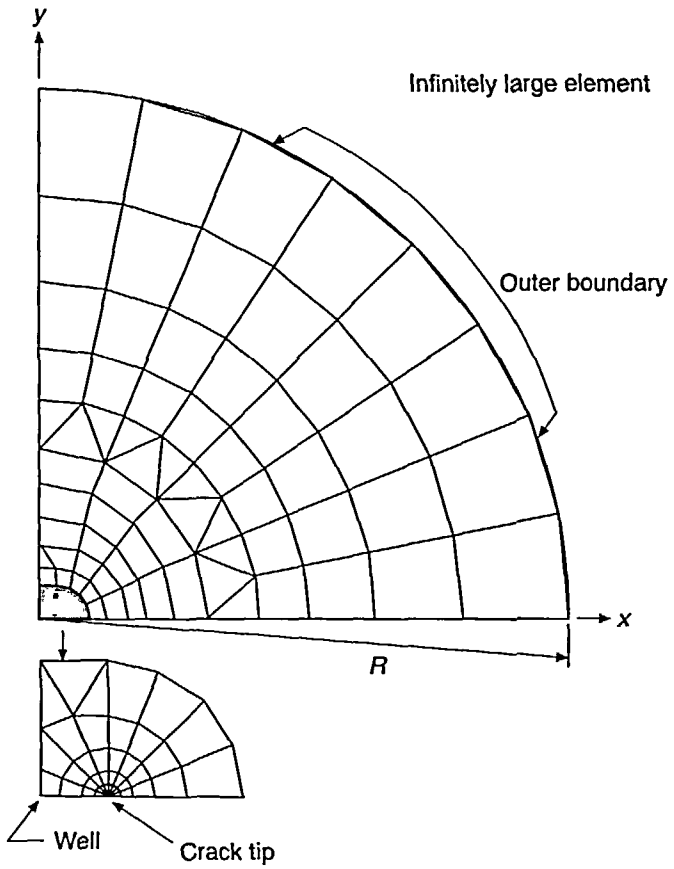

Figure 4 Finite element mesh for the problem of a slot in an infinite medium

$$\frac{\partial \phi}{\partial t} = a_0\phi + a_{-1}\phi_{-1} + a_{-2}\phi_{-2} \tag{27}$$

where

$$a_0 = \frac{2\Delta_{-1} + \Delta_{-2}}{\Delta_{-1}(\Delta_{-1} + \Delta_{-2})}$$

$$a_{-1} = -\frac{\Delta_{-1} + \Delta_{-2}}{\Delta_{-1}\Delta_{-2}}$$

$$a_{-2} = \frac{\Delta_{-1}}{\Delta_{-2}(\Delta_{-1} + \Delta_{-2})}$$

are three coefficients depending on the two-backward time increments Δ_{-1} and Δ_{-2}. Subscripts –1 and –2 denote the values of the physical quantities at time $t - \Delta_{-1}$ and $t - \Delta_{-1} - \Delta_{-2}$ respectively. The diffusion equation (12) is then equivalent to the variational equation:

$$\delta \Pi = 0 \tag{28}$$

where Π is the variational functional, which is:

$$\Pi = \int_{C_v} \phi \frac{\partial \phi^*}{\partial n} \, ds - \frac{1}{2} \iint_A \left[\left(\frac{\partial \phi}{\partial x} \right)^2 + \left(\frac{\partial \phi}{\partial y} \right)^2 + \frac{a_0}{\kappa} \phi^2 \right] dA$$

$$- \frac{1}{\kappa} \iint_A \phi (a_{-1} \phi_{-1} + a_{-2} \phi_{-2}) \, dA \tag{29}$$

where $\frac{\partial \phi^*}{\partial n}$ is the prescribed normal derivative of ϕ and n stands for the outer normal of the boundary. C_v stands for the portion of the boundary where the velocity of flow is prescribed. The value of ϕ has to be equal to the prescribed value ϕ^* on the boundary C_ϕ.

Figure 4 shows the finite element mesh for the problem. Because of the symmetry of the domain, only the first quadrant is considered. The outer boundary of the domain is chosen to be a constant ξ-curve. For the element within the sufficiently large domain, the value of ϕ in the elements are expressed by a regular four-node isoparametric interpolation of their nodal values. The region beyond the finite domain is occupied by an infinitely large element with a single degree of freedom, whose extrapolation function of ϕ is taken to be:

$$\phi - \phi_0 = \frac{\mathrm{Ei}\left(\frac{e^{2\xi}}{16 t_D} \right)}{\mathrm{Ei}\left(\frac{e^{2\bar{\xi}}}{16 t_D} \right)} (\bar{\phi} - \phi_0) \tag{30}$$

where $\bar{\xi}$ and $\bar{\phi}$ are, respectively, the values of ξ and ϕ on the outer boundary of the finite domain (*Figure 4*). Note that the boundaries of the finite elements, which share the outer boundary of the finite domain, do not coincide with the inner boundary of the infinitely large element since the outer boundary of the finite domain, the constant ξ-curve, is replaced by a broken line. However, our experience in finite element analysis tells us that this difference only results in a negligible error. It is obvious that equation (30) satisfies the condition of $\phi(\bar{\xi}) = \bar{\phi}$ and the limiting condition, equation (20). Furthermore, equation (30) simulates the distribution of ϕ for sufficiently large ξ as shown in equation (21). Therefore, the shape function of the infinitely large element can be set to be:

$$N(\xi, t) = \frac{\mathrm{Ei}\left(\frac{e^{2\xi}}{16 t_D} \right)}{\mathrm{Ei}\left(\frac{e^{2\bar{\xi}}}{16 t_D} \right)} \tag{31}$$

In forming the elemental coefficient matrix for the infinite element, the following integrals have been carried out:

$$\int_{\bar{\xi}}^{\infty} \left(\frac{\partial N}{\partial \xi}\frac{\partial \xi}{\partial x}\right)^2 |J|\, d\xi\,, \quad \int_{\bar{\xi}}^{\infty} \left(\frac{\partial N}{\partial \xi}\frac{\partial \xi}{\partial y}\right)^2 |J|\, d\xi\,,$$

$$\int_{\bar{\xi}}^{\infty} N^2 |J|\, d\xi\,, \quad \int_{\bar{\xi}}^{\infty} NN_{-1} |J|\, d\xi\,, \quad \int_{\bar{\xi}}^{\infty} NN_{-2} |J|\, d\xi$$

where $|J|$ is a Jacobi determinant approximated by:

$$|J| = L^2(\sinh^2\xi + \sin^2\eta) \simeq L^2\sinh^2\xi \simeq \frac{1}{4}L^2 e^{2\xi}\,, \qquad \text{for large } \xi$$

Because of the single degree of freedom, the elemental coefficient matrix of the infinite element reduces to a scalar, which will be assembled into the global coefficient matrix of the finite element equations. The variation equation (28) is then converted to a set of algebraic equations.

If the applied pressure ϕ_w on the slot surface is uniform and the flow rate q at the well bore is prescribed, the first term in the functional, equation (29), can be easily proved to be:

$$\int_{C_v} \phi \frac{\partial \phi^*}{\partial n}\, ds = 0.25\phi_w \frac{q}{K} \tag{32}$$

where q is defined positive for flowing from the well bore into the fracture. The coefficient 0.25 stems from the fact that only the first quadrant of the finite domain is considered. C_v is the slot surface in this case. K is the permeability of the reservoir. Through the variational equation (28), this term becomes $0.25\,(q/K)\delta\phi_w$ for prescribed flow rate q at the well bore. The term $0.25q/K$ will be added to the right-hand side of the finite element equation corresponding to the degree of freedom of the node at the well bore. The applied pressure ϕ_w can be obtained in the solution of the finite element equations.

If the applied pressure ϕ_w at the well bore is prescribed, the finite element equation corresponding to the degree of freedom of the node at the well bore will be modified in dealing with the constraint condition at the well bore. However, the flow rate q can be found by substituting the solution of ϕ into the equation, namely:

$$q = 4K\frac{\partial}{\partial \phi_w}\left\{\frac{1}{2}\iint_A \left[\left(\frac{\partial \phi}{\partial x}\right)^2 + \left(\frac{\partial \phi}{\partial y}\right)^2 + \frac{a_0}{\kappa}\phi^2\right] dA \right.$$

$$\left. + \frac{1}{\kappa}\iint_A \phi(a_{-1}\phi_{-1} + a_{-2}\phi_{-2})\, dA \right\} \tag{33}$$

where ϕ, ϕ_{-1} and ϕ_{-2} have been discretized in the finite element method.

The result of the dimensionless applied pressure ϕ_{wD} on the slot surface for the case of the prescribed flow rate is then plotted and compared with the exact analytical solution (*Figure 3*). An excellent agreement between them can be seen. In the case of prescribed applied pressure ϕ_w, the dimesionless flow rate at the well bore q_D is plotted and compared with the exact solutions (*Figure 2*). Amazingly, the two curves almost completely coincide.

Second, the infinite element method is used to analyse the transient pressure behaviour of a well intersected by a vertical finite conductivity fracture in an infinite slab reservoir. The fracture has a constant width b_f and an impermeable crack tip. Material in the fracture has a higher permeability than that in the reservoir. Cinco-Ley *et al.*[4] presented a semi-analytical solution for this problem. Li and Huang[3] also studied this problem by means of the finite element method (FEM) with an extrapolation technique. Owing to the narrow crack, flow in the fracture can be considered to be one-dimensional. Thus, the governing equation in the conductive fracture is:

$$b_f\left(-K_f\frac{\partial^2\phi}{\partial x^2}+c_f\frac{\partial\phi}{\partial t}\right)+2v_n=0 \tag{34}$$

where K_f is the permeability of the material in the fracture, and c_f is the compressibility of the fluid in the fracture. In Cinco-Ley *et al.*'s[4] work, the fluid in the fracture is considered to be incompressible, thus $c_f = 0$. v_n is the leak-off velocity, which is defined positive for outward flow of fluid from the fracture into the reservoir. Based on this definition, we have:

$$v_n = K\frac{\partial\phi^*}{\partial n}, \qquad \text{on fracture surface } C_v \tag{35}$$

According to equation (34), the leak-off velocity can be determined as:

$$v_n=\frac{1}{2}b_fK_f\frac{\partial^2\phi}{\partial x^2} \tag{36}$$

With the use of equations (35) and (36), the variation of the first integral of function Π in equation (29) becomes

$$\delta I=\int_{C_v}\delta\phi\frac{\partial\phi^*}{\partial n}\mathrm{d}s=\frac{b_fK_f}{2K}\int_{C_v}\delta\phi\frac{\partial^2\phi}{\partial x^2}\mathrm{d}x$$

Employing integration by parts, we obtain

$$\delta I=\frac{b_fK_f}{2K}\left[\delta\phi\frac{\partial\phi}{\partial x}\Big|_0^L-\int_{C_v}\frac{\partial\phi}{\partial x}\frac{\partial\delta\phi}{\partial x}\,\mathrm{d}x\right]$$

For the impermeable crack tip, we have $\frac{\partial\phi}{\partial x}\big|_{x=L}=0$. At the well bore, we have $\phi=\phi_w$ and

$$b_fK_f\frac{\partial\phi}{\partial x}\Big|_{x=0}=\frac{q}{2} \tag{37}$$

Thus, the variation of integral I becomes:

$$\delta I=\frac{1}{4K}\delta\left[\phi_wq-b_fK_f\int_{C_v}\left(\frac{\partial\phi}{\partial x}\right)^2\mathrm{d}x\right] \tag{38}$$

If triangular elements or four-node isoparametric elements share the crack boundary C_v, the pressure ϕ can be linearly distributed in an interval between a pair of nodal points on the crack surface. Hence, the integral in the second term of equation (38) can be discretized as:

$$\int_{C_v}\left(\frac{\partial\phi}{\partial x}\right)^2\mathrm{d}x=\sum_{i=1}^{n}\left[\phi^{(i-1)}\ \phi^{(i)}\right]\frac{1}{l_i}\begin{bmatrix}1&-1\\-1&1\end{bmatrix}\begin{Bmatrix}\phi^{(i-1)}\\\phi^{(i)}\end{Bmatrix} \tag{39}$$

where l_i is the length of the i-th interval, the superscripts (i) and $(i-1)$ denote the two ends of the interval and n is the total number of the intervals on the crack surface. Equation (39) is in a format ready for assembling into the global finite element coefficient matrix. The first term in equation

(38) can be used to deal with the boundary condition for either prescribed ϕ_w or q at the well bore. The flow rate for given ϕ_w can be determined by:

$$q = 4K\frac{\partial}{\partial \phi_w}\left\{\frac{1}{2}\iint_A \left[\left(\frac{\partial \phi}{\partial x}\right)^2 + \left(\frac{\partial \phi}{\partial y}\right)^2 + \frac{a_0}{\kappa}\phi^2\right] dA + \frac{1}{\kappa}\iint_A \phi(a_{-1}\phi_{-1} + a_{-2}\phi_{-2})dA + \frac{b_f K_f}{4K}\int_{C_v}\left(\frac{\partial \phi}{\partial x}\right)^2 dx\right\} \quad (40)$$

It can be seen in equation (40) that one more term is added to equation (33).

Results for the dimensionless pressure ϕ_{wD} at the well bore with the use of this method are plotted against the dimensionless time t_D and compared with those of Cinco-Ley*et al.*[4] as shown in *Figure 5*, where the parameter F_D is called dimensionless fracture conductivity and defined by:

$$F_D = \frac{b_f K_f}{LK} \quad (41)$$

A large value of F_D represents a highly conductive fracture. In *Figure 5*, our results and Cinco-Ley's results are in good agreement for $F_D = \pi$ and 100π. Our results for $F_D = 0.2\pi$ have a slightly larger difference from Cinco-Ley's results. However, it can be seen in *Figure 5* that the curves plotted for the two results are parallel to each other. Furthermore, our results are very close to those presented by Li and Huang[3] for $F_D = 0.2\pi$.

Cinco-Ley[4] did not give the solution of q for prescribed applied pressure at the well bore. The solution is presented here as a complement (*Figure 6*). According to Cinco-Ley *et al.*'s results of ϕ_{wD} for prescribed flow rate q, solution for $F_D = 100\pi$ is very close to Kucuk and Bingham's[2] solution for an empty fracture. The complemented results for $F_D = 100\pi$ are also in excellent

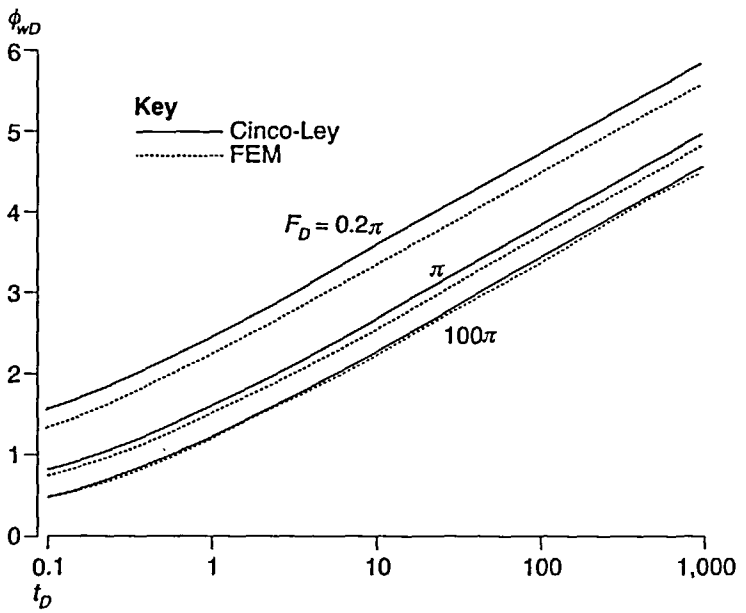

Figure 5 Comparison of the results of the FEM employing an infinitely large element with those by Cinco-Ley *et al.*[4] for the case of a finite conductivity fracture in an infinite medium

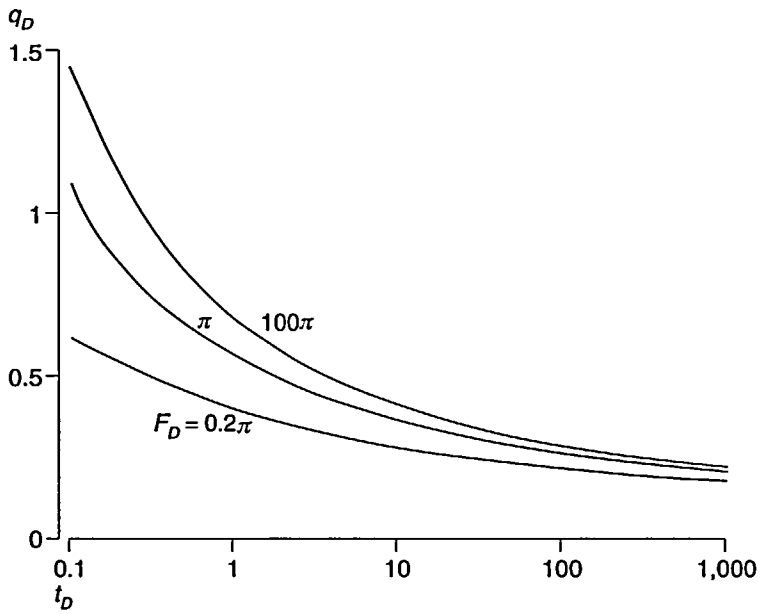

Figure 6 Flow rate q_D at the well bore vs time t_D for the case of a finite conductivity fracture in an infinite medium with a prescribed constant applied pressure at the well bore

agreement with Kucuk and Bingham's results. Hence, the solutions in lower conductivity fracture cases such as $F_D = \pi$ and $F_D = 0.2\pi$ can be considered correct.

A sensitivity analysis has been conducted in order to estimate a proper size for the sufficiently large domain. Initially, the ratio of the average radius of the finite domain to the half crack length R/L is about 50 in our calculation. Afterwards, the elements, which share the outer boundary, are removed layer by layer. It is found that the solution does not change appreciably when the ratio R/L is equal to or large than 16 (*Figure 7*). Results also indicated that the solutions are accurate enough for practical purposes if at least $R/L = 10$ is considered. Therefore, this infinite element method is proved to be quite effective.

AN EXAMPLE

Consider a fully penetrating vertical fracture of length $2L$ in an infinitely large slab reservoir with a well located at the centre of the fracture. The size of the well is neglected in comparison with the fracture length. The basic equation governing the transient pressure behaviour in the finite conductivity fracture is shown as equation (34). However, in this equation the width of fracture b_f is a function of x for the elliptically-shaped conductive fracture. With the use of equations (34) and (35), the variation of the first integral of Π gives:

$$\delta I = \int_{C_v} \delta\phi \frac{\partial \phi^*}{\partial n} \mathrm{d}s$$

$$= \frac{1}{2K} \left\{ K_f \left[\left(b_f \delta\phi \frac{\partial \phi}{\partial x} \right) \Big|_0^L - \int_{C_v} \frac{\partial \phi}{\partial x} \frac{\partial \delta(b_f \phi)}{\partial x} \mathrm{d}x \right] \right.$$

$$\left. - \int_{C_v} b_f c_f \delta\phi (a_0\phi + a_{-1}\phi_{-1} + a_{-2}\phi_{-2}) \mathrm{d}x \right\} \tag{42}$$

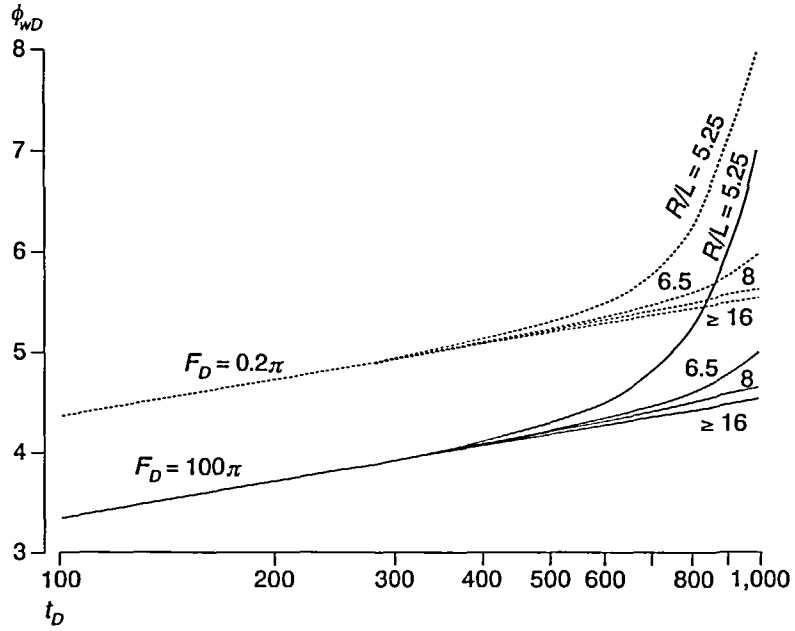

Figure 7 Sensitivity analysis of the infinitely large element method

where $b_f = 0$ at the crack tip $x = L$. The pore pressure ϕ in each interval can be expressed by a linear interpolation function of its nodal values. Since b_f in each fracture interval weakly depends on x, the average value of the crack width $b_f^{(i)}$ can be used to approximate the crack width of the i-th interval. Hence, equation (42) can be partitioned as:

$$\delta I = \frac{1}{4K}\delta\ (\phi_w q - K_f \sum_{i=1}^{n} [\phi^{(i-1)}\ \phi^{(i)}] \frac{b_f^{(i)}}{l_i} \begin{bmatrix} 1 & -1 \\ -1 & 1 \end{bmatrix} \begin{Bmatrix} \phi^{(i-1)} \\ \phi^{(i)} \end{Bmatrix}$$

$$- c_f \sum_{i=1}^{n} b_f^{(i)} l_i a_0 [\phi^{(i-1)}\ \phi^{(i)}] \begin{bmatrix} 1/3 & 1/6 \\ 1/6 & 1/3 \end{bmatrix} \begin{Bmatrix} \phi^{(i-1)} \\ \phi^{(i)} \end{Bmatrix}$$

$$- 2c_f \sum_{i=1}^{n} b_f^{(i)} l_i [\phi^{(i-1)}\ \phi^{(i)}] \begin{bmatrix} 1/3 & 1/6 \\ 1/6 & 1/3 \end{bmatrix} \begin{Bmatrix} a_{-1}\phi_{-1}^{(i-1)} + a_{-2}\phi_{-2}^{(i-1)} \\ a_{-1}\phi_{-1}^{(i)} + a_{-2}\phi_{-2}^{(i)} \end{Bmatrix} \ ) \qquad (43)$$

where $\delta\phi_w = 0$ at $x = 0$ if the pore pressure at the well bore is prescribed. Equation (43) can be imposed by the global finite element equations.

The following material and geometrical constants are employed for the reservoir and the finite conductivity fracture in our computation:

$$K = 4.453\times10^{-5}\text{ft}^2\text{psf}^{-1}\text{day}^{-1},\ c = 0.34\times10^{-8}\text{psi}^{-1},\ \kappa = 13.1\times10^{3}\text{ft}^2\text{day}^{-1},$$

$$K_f = 0.04453\ \text{ft}^2\text{psf}^{-1}\text{day}^{-1},\ c_f = 0.34\times10^{-8}\text{psi}^{-1},\ L = 100\ \text{ft}$$

The *in situ* stress components are $\sigma_x^{\infty} = -2{,}000$psi and $\sigma_y^{\infty} = -1{,}500$psi (compression), and the initial pore pressure in the reservoir is $\phi_0 = 800$psi. The pressure applied to the well exceeds the *in situ* stress by 150.5psi, generating a crack with a crack-mouth-opening displacement of one third

of an inch at the well bore. As it drops to 100psi afterwards, the opened crack is retained by the sand in the fracture. This procedure of crack opening and sand filling is completed in such a short time that it may be assumed to take place instantly. Thus, the problem consists of two steps as shown in *Figure 8*. In the first step (*Figure 8(a)*), an inner pressure ϕ_i = 1,650.5psi is applied to the crack surface. This step can be regarded as a superposition of two problems. The first problem has the solution of a uniform stress field with σ_x = –2,000psi, σ_y = –1,500psi and τ_{xy} = 0, and a uniform pore pressure field with ϕ = 800psi. In the second problem, the pore pressure is zero elsewhere except at the crack surface, where the pore pressure is 850.5psi. In the second step (*Figure 8(b)*), the applied inner pressure drops to 100psi and the crack is filled with sand. This step can also be divided into two problems. Although the geometry and loading condition are different from those in the first step, the solution of the first problem of the second step still gives uniform fields of stress and pore pressure which are the same as in the first step. Based on this analysis, the initial condition and boundary condition for pore pressure of the second problem of the second step are:

$$\phi_0 = \begin{cases} 850.5 \text{ psi} & \text{on fracture surface } C_v \\ 0 & \text{elsewhere} \end{cases}$$

and

ϕ_w = –700 psi at the well bore

The final solution of the second step can be obtained by superposition of these two problems.

An uncoupled problem is considered, namely, the influence of the deformation on the transient pressure behaviour is neglected. The finite element mesh is shown in *Figure 4*. The flow rate at the well bore can be determined by:

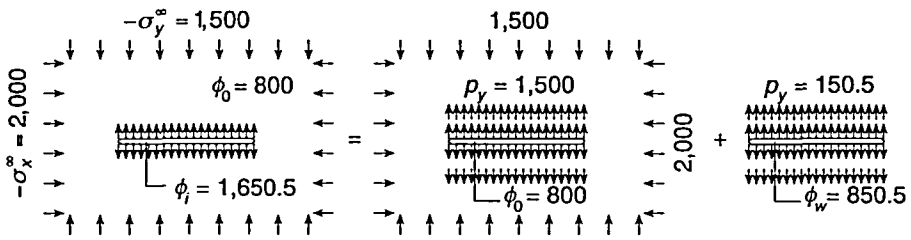

(a) The first step: an inner pressure ϕ_i = 1,650.5 psi is applied

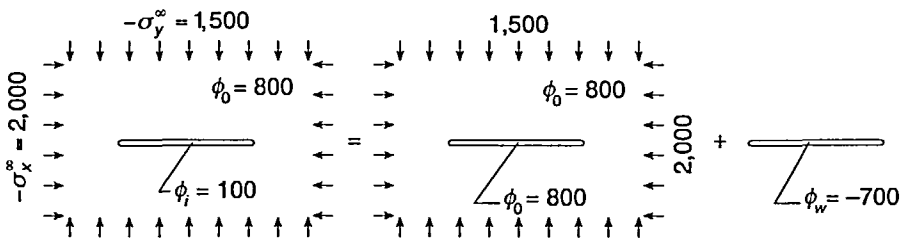

(b) The second step: the applied pressure ϕ_i drops to 100psi

Figure 8 Illustration of the superposition method for the problem of a single well in an infinite medium with a conductive fracture

$$q = 4K\frac{\partial}{\partial \phi_w}\left\{ \frac{1}{2}\iint_A \left[\left(\frac{\partial \phi}{\partial x}\right)^2 + \left(\frac{\partial \phi}{\partial y}\right)^2 + \frac{a_0}{K}\phi^2\right] dA \right.$$

$$+ \frac{1}{K}\iint_A \phi(a_{-1}\phi_{-1} + a_{-2}\phi_{-2})dA + \frac{K_f}{4K}\int_{C_v} b_f\left(\frac{\partial \phi}{\partial x}\right)^2 dx$$

$$\left. + \int_{C_v} b_f c_f \left[\frac{1}{2}a_0\phi^2 + \phi\,(a_{-1}\phi_{-1} + a_{-2}\phi_{-2})\right] dx \right\} \tag{44}$$

The numerical results are shown in *Figures 9-11*. *Figure 9* shows that the production rate decreases with increasing time if the applied pressure at the well bore is kept constant. The pore pressure distribution on the fracture and the x-axis are shown in *Figures 10* and *11*, which indicate that the pore pressure approaches the initial value when the material point gets further from the fracture.

DISCUSSION AND CONCLUSION

There are three ways to determine the flow rate at the well bore for the finite conductivity fracture problem.

(1) The leak-off velocity v_n can be calculated with equation (35). The flow rate at the well bore is the integral of the leak-off velocity along the crack surface.

(2) The flow rate can be determined by equation (37).

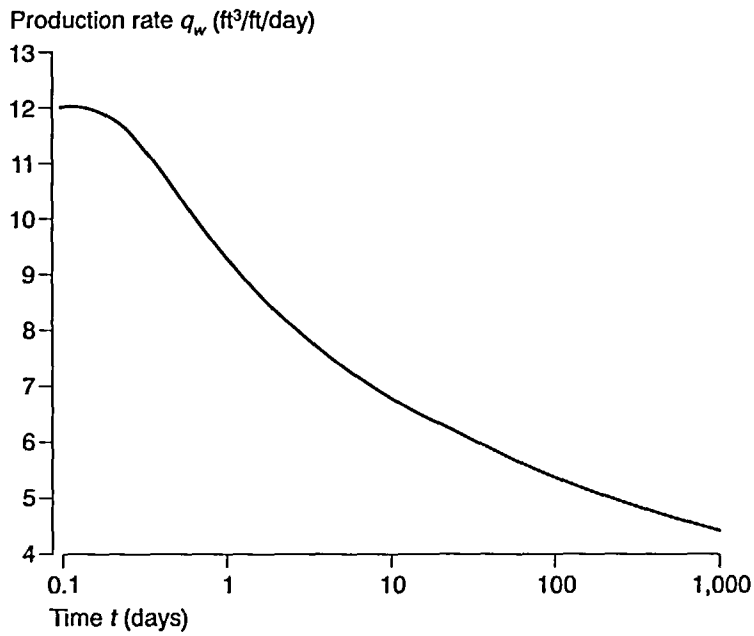

Figure 9 Curves of production rate q_w vs time t for the example

(3) The flow rate can be determined by equations (33), (40) or (44). In fact, these equations mean that the term $0.25q/K$ is the difference between the left-hand side and the right-hand side of the finite element equation corresponding to the degree of freedom of the nodal point at the well bore.

It is well-known that numerical derivatives generally contain larger errors. Hence, the second method has the largest errors because the flow rate depends on a numerical derivative at a single node at the well bore. Errors of the first method are next to the second. The flow rate depends on

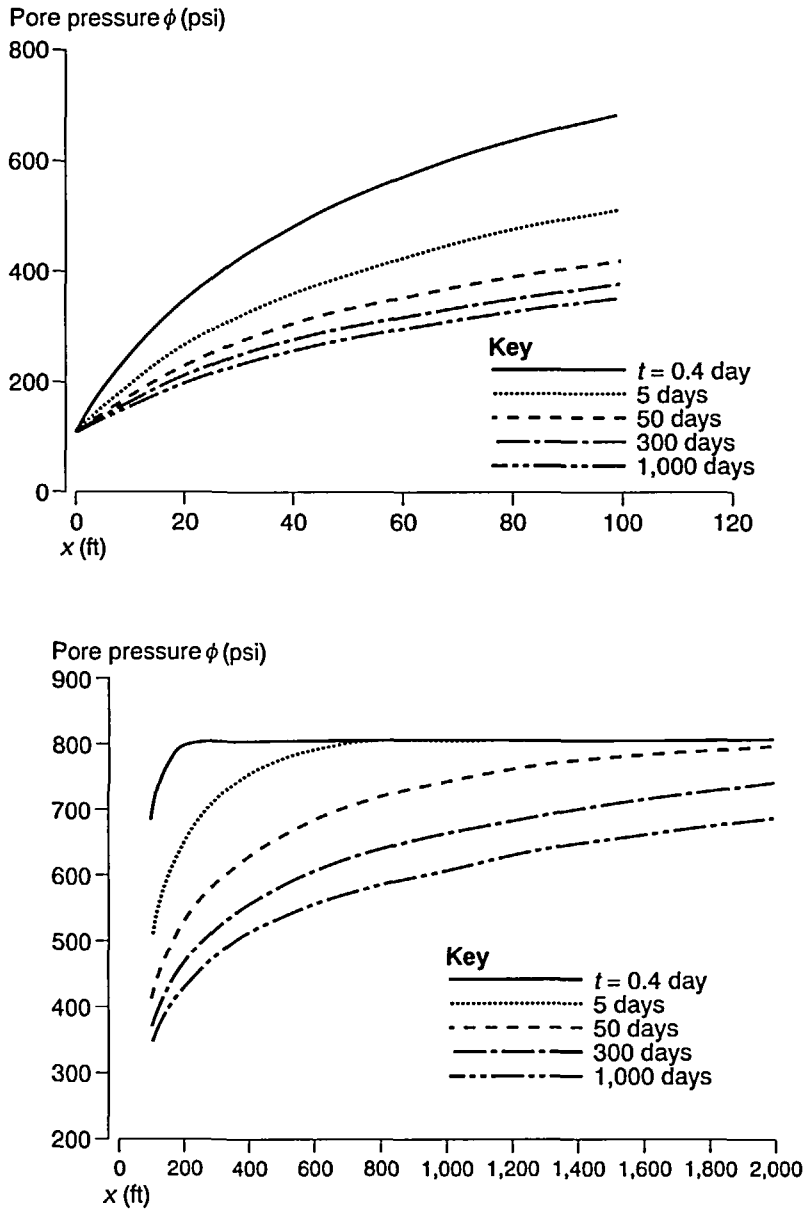

Figure 11 Distribution of the pore pressure ϕ on the x-axis for the example

the derivatives at several nodal points on the fracture surface and, finally, the flow rate is obtained by numerical integral. So, errors may be eliminated somehow. The third method has the highest accuracy since numerical derivatives never occur there. The computation demonstrates that the numerical results from the first and the third methods are close. However, large differences are found between the results from the second and the third methods. In *Figure 2*, it is noted that the numerical results of the flow rate in the third method for an empty fracture are almost the same as those of Kucuk and Brigham's[2] exact solution. Therefore, the third method can be considered reliable.

In this work, the approximate analytical solutions for two kinds of diffusion problems are presented. One of them is for the case of a single cylindrical well in an infinite medium, and the other is for the case of a slot in an infinite medium. Both solutions approach the exact solutions for sufficiently large time or distance from the material point to the internal boundary. The latter is applied to develop infinite elements for analysing seepage problems for a well in an infinitely large medium with a finite conductivity fracture. Comparison of the numerical results with the theoretical results by Kucuk and Brigham's and the semi-analytical results by Cinco-Ley *et al.*[4] demonstrate good accuracy and reliability. Sensitivity analysis shows a high effectiveness of this method.

The purpose of developing the infinite elements is to analyse transient pressure behaviour of a hydraulically fractured well in an infinitely extended reservoir in a more complex case. An example of a transient pressure behaviour problem for an elliptically-shaped finite conductivity fracture in an infinite slab reservoir with the use of this infinite element method is presented. The effectiveness and accuracy of this method can be seen through this example. This method even can be used to solve the problem of time-dependent applied pressure or flow rate applied at the well bore, and the problem of hydraulic fracture propagation, etc.

ACKNOWLEDGEMENTS

This work is co-sponsored by research grants Z93(034) from Shanghai Tiedao University and the Science Foundation G95(02) from State Education Committee of the People's Republic of China.

REFERENCES

1 Jaeger, J.C., Numerical values for the temperature in radial heat flow, *J. Math. Phys.*, **34**, 316-321 (1955)
2 Kucuk, F. and Brigham, W.E., Transient flow in elliptic systems, *Soc. Petrol. Eng. J.*, 401-410 (December 1979)
3 Li, Y.C. and Huang, N.C., Flow field modelling near a well with a conductive fracture, *Int.J. Num. Meth. in Fluids*, **15**, 545-569 (1992)
4 Cinco-Ley, H., Samaniego, V.F. and Dominguez, N., Transient pressure analysis for a well with finite conductivity fracture, *Soc. Petrol. Eng., J.*, 253-264 (August 1978)
5 Bettess, P,. Infinite elements, *Int. J. Num. Meth. Eng.*, **11**, 53-64 (1977)
6 Bettess, P. and Zienkiewicz, O.C., Diffraction and refraction of surface waves using finite and infinite elements, *Int. J. Num. Meth. Eng.*, **11**, 1271-1290 (1977)
7 Anderson, D.L. and Ungless, R.L., Infinite finite elments, *Int. Symp. Innovative Num. Anal. Appl. Eng. Sci.*, France (1977)
8 Gartling, D. and Becker, E.B., Computationally efficient finte element analysis of viscous flow problems, in Oden, J.T. *et al.*, Eds, *Computational Methods in Non Linear Mechanics*, Texas Institute for Computational Mechanics (1974), *Proceedings of the International Conference on Computational Methods in Non Linear Mechanics*, held at the University of Texas, Austin, Texas, 23-25 September (1974)
9 Lynn, P.P. and Hadid, H.A., Infinite elements with $1/r^n$ type decay, *Int. J. Num. Meth. Eng.*, **17**, 347-355 (1981)
10 Chow, Y.K. and Smith, I.M., Static and periodic infinite solid elements, *Int. J. Num. Meth. Eng.*, **17**, 503-526 (1981)
11 Askar, H.G. and Lynn, P.P., Infinite elements for ground freezing problems, *Journal of Engineering Mechanics*, Proc. ASCE, **110**, 157-172 (1984)
12 Beer, G. and Meek, J.L., Infinite domain elements, *Int. J. Num. Meth. Eng.*, **17**, 43-52 (1981)
13 Domjanic, F. and Owen, D.R.J. Mapped infinite elements in transient thermal analysis, *Computers and Structures*, **19**, 673-687 (1984)
14 Simoni, L. and Schrefler, B.A. Mapped infinite elements in soil consolidation, *Int. J. Num. Meth. Eng.*, **24**, 513-527 (1987)
15 Simoni, L. and Schrefler, B.A. Numerical modelling of unbounded domains in coupled field problems, *Meccanica (Journal of the Italian Association of Theoretical and Applied Mechanics)*, **24**, 98-105 (1989)